

University of Texas Rio Grande Valley

ScholarWorks @ UTRGV

---

Earth, Environmental, and Marine Sciences  
Faculty Publications and Presentations

College of Sciences

---

11-16-2019

## Investigations of Aerobic Methane Oxidation in Two Marine Seep Environments: Part 1—Chemical Kinetics

Eric W. Chan

*The University of Texas Rio Grande Valley*

Allan M. Shiller

*University of Southern Mississippi*

Dongjoo J. Joung

*University of Southern Mississippi*

Eleanor C. Arrington

*University of California, Santa Barbara*

David L. Valentine

*University of California, Santa Barbara*

*See next page for additional authors*

Follow this and additional works at: [https://scholarworks.utrgv.edu/eems\\_fac](https://scholarworks.utrgv.edu/eems_fac)



Part of the [Earth Sciences Commons](#), [Environmental Sciences Commons](#), [Marine Biology Commons](#), and the [Oceanography and Atmospheric Sciences and Meteorology Commons](#)

---

### Recommended Citation

Chan, E. W., A. M. Shiller, D. J. Joung, E. C. Arrington, D. L. Valentine, M. C. Redmond, J. A. Breier, S. A. Socolofsky, and J. D. Kessler. 2019. "Investigations of Aerobic Methane Oxidation in Two Marine Seep Environments: Part 1—Chemical Kinetics." *Journal of Geophysical Research: Oceans* 124 (12): 8852–68. <https://doi.org/10.1029/2019JC015594>.

This Article is brought to you for free and open access by the College of Sciences at ScholarWorks @ UTRGV. It has been accepted for inclusion in Earth, Environmental, and Marine Sciences Faculty Publications and Presentations by an authorized administrator of ScholarWorks @ UTRGV. For more information, please contact [justin.white@utrgv.edu](mailto:justin.white@utrgv.edu), [william.flores01@utrgv.edu](mailto:william.flores01@utrgv.edu).

---

**Authors**

Eric W. Chan, Allan M. Shiller, Dongjoo J. Joung, Eleanor C. Arrington, David L. Valentine, Molly C. Redmond, John A. Breier, Scott A. Socolofsky, and John D. Kessler

## RESEARCH ARTICLE

10.1029/2019JC015594

This article is a companion to Chan et al. (2019) <https://doi.org/10.1029/2019JC015603>.

## Key Points:

- Aerobic methane oxidation was investigated and showed that two moles of oxygen are not required to oxidize one mole of methane
- After a lag time lasting days to weeks, methane was rapidly oxidized in a few days following first-order chemical kinetics
- These results appear consistent between different oceanic environments, despite regional variabilities

## Supporting Information:

- Supporting Information S1

## Correspondence to:

E. W. Chan and J. D. Kessler,  
john.kessler@rochester.edu;  
erik.w.chan@gmail.com

## Citation:

Chan, E. W., Shiller, A. M., Joung, D. J., Arrington, E. C., Valentine, D. L., Redmond, M. C., et al. (2019). Investigations of aerobic methane oxidation in two marine seep environments: Part 1—Chemical kinetics. *Journal of Geophysical Research: Oceans*, 124. <https://doi.org/10.1029/2019JC015594>

Received 29 AUG 2019

Accepted 25 OCT 2019

Accepted article online 16 NOV 2019

## Investigations of Aerobic Methane Oxidation in Two Marine Seep Environments: Part 1—Chemical Kinetics

E. W. Chan<sup>1,6</sup> , A. M. Shiller<sup>2</sup> , D. J. Joung<sup>2</sup> , E. C. Arrington<sup>3</sup> , D. L. Valentine<sup>4</sup> , M. C. Redmond<sup>5</sup> , J. A. Breier<sup>6</sup> , S. A. Socolofsky<sup>7</sup> , and J. D. Kessler<sup>1</sup> 

<sup>1</sup>Department of Earth and Environmental Sciences, University of Rochester, Rochester, NY, USA, <sup>2</sup>Division of Marine Science, University of Southern Mississippi, Stennis Space Center, MS, USA, <sup>3</sup>Interdepartmental Graduate Program in Marine Science, University of California, Santa Barbara, CA, USA, <sup>4</sup>Department of Earth Science and Marine Science Institute, University of California, Santa Barbara, CA, USA, <sup>5</sup>Department of Biological Sciences, University of North Carolina at Charlotte, Charlotte, NC, USA, <sup>6</sup>School of Earth, Environment, and Marine Sciences, University of Texas Rio Grande Valley, Brownsville, TX, USA, <sup>7</sup>Zachry Department of Civil Engineering, Texas A&M University, College Station, TX, USA

**Abstract** Microbial aerobic oxidation is known to be a significant sink of marine methane (CH<sub>4</sub>), contributing to the relatively minor atmospheric release of this greenhouse gas over vast stretches of the ocean. However, the chemical kinetics of aerobic CH<sub>4</sub> oxidation are not well established, making it difficult to predict and assess the extent that CH<sub>4</sub> is oxidized in seawater following seafloor release. Here we investigate the kinetics of aerobic CH<sub>4</sub> oxidation using mesocosm incubations of fresh seawater samples collected from seep fields in Hudson Canyon, U.S. Atlantic Margin and MC118, Gulf of Mexico to gain a fundamental chemical understanding of this CH<sub>4</sub> sink. The goals of this investigation were to determine the response or lag time following CH<sub>4</sub> release until more rapid oxidation begins, the reaction order, and the stoichiometry of reactants utilized (i.e., CH<sub>4</sub>, oxygen, nitrate, phosphate, trace metals) during CH<sub>4</sub> oxidation. The results for both Hudson Canyon and MC118 environments show that CH<sub>4</sub> oxidation rates sharply increased within less than one month following the CH<sub>4</sub> inoculation of seawater. However, the exact temporal characteristics of this more rapid CH<sub>4</sub> oxidation varied based on location, possibly dependent on the local circulation and biogeochemical conditions at the point of seawater collection. The data further suggest that methane oxidation behaves as a first-order kinetic process and that the reaction rate constant remains constant once rapid CH<sub>4</sub> oxidation begins.

**Plain Language Summary** In and below the seafloor resides the largest global reservoir of methane, a potent greenhouse gas. Following the release of methane from the seafloor, a significant fraction dissolves in the overlying seawater and is oxidized by indigenous microorganisms, helping to prevent its atmospheric release. However, the timing and chemical requirements for this process to occur are not well established, making it difficult to predict and assess the efficiency of methane oxidation following seafloor release. This study systematically measured the chemical changes that are associated with aerobic methane oxidation in seawater using water collected from regions of active seafloor methane release along the U.S. Atlantic margin and the Gulf of Mexico. These results help to refine our understanding of how quickly and how much methane can typically be oxidized in seawater.

### 1. Introduction

The atmospheric concentration of methane (CH<sub>4</sub>) has increased by a factor of 2.5 from preindustrial levels of ~700 to 1,850 ppb today, showing the importance of determining the sources and sinks of this greenhouse gas (Dlugokencky et al., 2011). While the oceans account for only ~1 to 3% (4–15 Tg yr<sup>-1</sup>) of all atmospheric sources of CH<sub>4</sub> today (Dlugokencky et al., 2011), the CH<sub>4</sub> sequestered in and below the seafloor forms the largest CH<sub>4</sub> reservoir on Earth, whose stability is in part controlled by temperature and pressure (Ruppel & Kessler, 2017). The oceanic CH<sub>4</sub> system is dynamic with formation mechanisms of CH<sub>4</sub> including thermogenic, biogenic, and abiogenic processes (e.g., Karl et al., 2008; Kelley & Früh-Green, 1999; Oremland & Taylor, 1978; Sherwood Lollar et al., 2002). While seafloor emissions are capable of releasing CH<sub>4</sub> from all of these sources to the overlying waters, the depth below the sea surface, the temperature of the

surrounding water, and total CH<sub>4</sub> concentration can cause CH<sub>4</sub> to be trapped in sediments as ice-like clathrate hydrates (Ruppel & Kessler, 2017). Nonetheless, globally significant releases of CH<sub>4</sub> carbon from the seafloor have been hypothesized to have occurred during the geologic past, influencing past climate, and possibly occur today (Ruppel & Kessler, 2017). For example, seafloor CH<sub>4</sub> releases are one possible explanation for the global change in carbon cycle dynamics at the Paleocene-Eocene Thermal Maximum (PETM; Dickens, 2011; Dickens et al., 1995; Higgins & Schrag, 2006; Zeebe et al., 2016). This hypothesis postulates that CH<sub>4</sub> hydrates were destabilized through deep-ocean warming and that the newly released CH<sub>4</sub> was oxidized in sediments and the overlying water column, injecting globally significant amounts of carbon into the active global carbon system (Dickens et al., 1995). In the modern ocean, seafloor CH<sub>4</sub> releases are likely not insignificant (Ruppel & Kessler, 2017), yet the relatively minimal emission of oceanic CH<sub>4</sub> to the atmosphere indicates active CH<sub>4</sub> oxidation in seawater (Reeburgh, 2007; Valentine, 2011).

The single largest seafloor CH<sub>4</sub> release that was directly observed occurred during the 2010 Deepwater Horizon (DWH) well blowout. In addition to oil, large quantities of CH<sub>4</sub> were emitted into the deep waters of the Gulf of Mexico during this incident, and measurements suggest that the released CH<sub>4</sub> was contained in intrusion layers in the deep Gulf waters (800–1,100 m) with minimal direct emission to the atmosphere (Camilli et al., 2010; Crespo-Medina et al., 2014; Kessler et al., 2011; Ryerson et al., 2012; Socolofsky et al., 2011; Valentine et al., 2010; Yvon-Lewis et al., 2011). Several studies investigated the microbial oxidation of released CH<sub>4</sub> in the Gulf waters during and following this release (Crespo-Medina et al., 2014; Du & Kessler, 2012; Dubinsky et al., 2013; Kessler et al., 2011; Rogener et al., 2018; Shiller et al., 2017; Valentine et al., 2010), as other work has shown aerobic CH<sub>4</sub> oxidation to be a substantial removal mechanism for CH<sub>4</sub> entering the ocean water column (e.g., de Angelis et al., 1993; Leonte et al., 2017; Mau et al., 2013; Pack et al., 2015; Valentine et al., 2001). Metatranscriptomes showed a clear increase in hydrocarbon monooxygenase gene expression in late May 2010, providing evidence that the oxidation of CH<sub>4</sub> and another low-molecular-weight alkane had already commenced at 30 days after the onset of the spill (Rivers et al., 2013), while Valentine et al. (2010) suggested that the oxidation of ethane and propane was occurring more rapidly than CH<sub>4</sub> in early June. Also, stable isotope probing experiments were carried out with DWH samples, indicating that methanotrophs responded more slowly compared to other organisms responsible for the oxidation of ethane, propane, and some higher molecular weight hydrocarbons (Redmond & Valentine, 2012).

Kessler et al. (2011) and Du and Kessler (2012) used the decrease in dissolved oxygen (DO) in the deepwater CH<sub>4</sub> and hydrocarbon intrusion layers as a tracer of CH<sub>4</sub> oxidation during the DWH incident and determined that the DO loss integrated over the entire plume area was sufficient to account for complete oxidation of released CH<sub>4</sub>. The Kessler et al. (2011) study also assembled a pseudo-first-order model to predict that the greatest amount of CH<sub>4</sub> oxidation (averaged over the entire deep-water plume) occurred ~60–120 days from the start of the spill, and the more comprehensive DO anomaly data set presented in Du and Kessler (2012) supported the timing of the predicted rapid CH<sub>4</sub> oxidation. Crespo-Medina et al. (2014) presented numerous measurements of CH<sub>4</sub> oxidation rates spanning this entire event, from spring through winter of 2010. The first-order oxidation rate constants produced from their CH<sub>4</sub> oxidation rate measurements (Crespo-Medina et al., 2014) generally support the predicted average values for first-order CH<sub>4</sub> oxidation rate constants (Kessler et al., 2011) up to 70 days after the start of the spill (Figure 1). However, many measured CH<sub>4</sub> oxidation rate constants do not agree with the model for times greater than 120 days after the spill when the dissolved CH<sub>4</sub> concentrations decreased significantly below values measured during active emission from the well. The model implicitly assumed that CH<sub>4</sub> oxidation rate constants were proportional to cell density or the activity of the microbial population involved in aerobic CH<sub>4</sub> oxidation, and thus would increase following CH<sub>4</sub> injection and decrease as the new microbial population was remineralized when CH<sub>4</sub> concentrations decreased (Kessler et al., 2011). However, the measurements suggested that the rate constants remain high following rapid CH<sub>4</sub> oxidation and only decrease over longer time scales (Crespo-Medina et al., 2014; Rogener et al., 2018; Figure 1). Unfortunately, only two CH<sub>4</sub> oxidation rate measurements were reported in the deep intrusion layer (800–1,100 m) during the ~60- to 120-day window when Kessler et al. (2011) predicted that the highest average amounts of CH<sub>4</sub> oxidation would occur, and the dates of collection for those two samples are uncertain (Crespo-Medina et al., 2014). Thus, the investigation presented here was initially motivated by the DWH blowout to provide empirical biogeochemical data to thoroughly

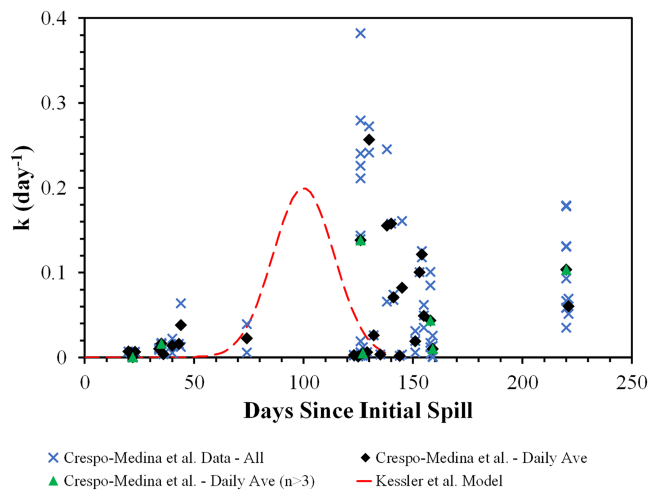


**Figure 1.** Predicted and measured first-order rate constants for the oxidation of  $\text{CH}_4$  released during the Deepwater Horizon blowout (DWH) in the Gulf of Mexico. Here we assume that  $\text{CH}_4$  oxidation rate constants vary proportionally to the cell density or activity of the microbial population involved in aerobic  $\text{CH}_4$  oxidation. Red dashed line = modeled change in  $\text{CH}_4$  oxidation rate constants averaged over the entire deepwater plume from Kessler et al. (2011). Blue cross = individual rate constants reported in Crespo-Medina et al. (2014) in the deep plume (800–1,100-m water depth). Black diamond = rate constants, averaged daily, reported in Crespo-Medina et al. (2014) in the deep plume (800–1,100-m water depth). Green triangle = rate constants, averaged daily when the number of data points in a specific day is  $>3$ , reported in Crespo-Medina et al. (2014) in the deep plume (800–1,100-m water depth). The vertical gray line represents the day the blowout was stopped and no longer emitting  $\text{CH}_4$ . The lack of empirical data is apparent between 60 and 120 days after the initiation of the spill when Kessler et al. (2011) predicted the greatest change in methane oxidation rate constants averaged over the entire deepwater plume.

characterize the temporal changes in microbial oxidation following a  $\text{CH}_4$  release. However, these experiments were designed to not only help interpret the fate of  $\text{CH}_4$  following the DWH blowout but also to provide more general information on the chemical kinetics of aerobic  $\text{CH}_4$  oxidation.

Here we conducted mesocosm experiments with  $\text{CH}_4$ -laden seawater while measuring the chemical changes over time during  $\text{CH}_4$  oxidation events. To assess regional variability in  $\text{CH}_4$  oxidation kinetics, seawater was collected in two different locations where  $\text{CH}_4$  bubbles were escaping the seafloor: (a) Hudson Canyon off the coast of New York and New Jersey near the upper limit of  $\text{CH}_4$  hydrate stability and (b) the deep Gulf of Mexico near waters once impacted by the DWH blowout (Figure 2). Two goals guided this investigation. The first goal was to determine the chemical kinetics for this oxidation reaction, which included the lag time, or the time between  $\text{CH}_4$  exposure and the onset of rapid consumption, and the reaction order. The second goal was to determine the stoichiometry of reactants utilized (i.e.,  $\text{CH}_4$ , oxygen, nitrate, phosphate, trace metals) during  $\text{CH}_4$  removal from seawater. The results of these studies can be used to predict the timing of and limitations on  $\text{CH}_4$  oxidation following natural or anthropogenic release based on the ambient concentrations of bioactive compounds.

## 2. Materials and Methods

Waters influenced by known  $\text{CH}_4$  seep activity were chosen to examine  $\text{CH}_4$  oxidation kinetics. The first research expedition was aboard the R/V *Endeavor* on the North Atlantic Bight from 7–12 July 2014 (Table 1 and Figure 2). The recently discovered  $\text{CH}_4$  seeps off the coast of New York and New Jersey in Hudson Canyon (HC; Rona et al., 2015; Skarke et al., 2014; Weinstein et al., 2016) provided an appropriate site for these experiments. Water samples were collected both inside the seep field as well as outside of HC in waters not directly impacted by  $\text{CH}_4$  seeps, as

determined by the presence or absence of acoustically detected bubbles (Leonte et al., 2017; Weinstein et al., 2016). The second research expedition was from 9–20 April 2015 aboard the E/V *Nautilus* at the Sleeping Dragon seep field site (MC118) in the Gulf of Mexico (Table 1 and Figure 2). MC118 is 17 km from the Deepwater Horizon wellhead and provided physical-chemical conditions similar to what may have been experienced during the DWH blowout in 2010. The results obtained from HC and MC118 were analyzed to determine regional similarities and variabilities in  $\text{CH}_4$  oxidation kinetics.

### 2.1. Incubation and Analysis System

A dissolved gas analyzer system (DGAS) and mesocosm incubation system (MIS) were recently developed (Chan et al., 2016) and were used here to measure the concentration and natural stable isotopes of gases dissolved in seawater throughout mesocosm incubation experiments. (The natural stable isotope results are presented in Chan et al., 2019.) In brief, the DGAS unit was developed for the automated analysis of seawater incubations at user-defined intervals, allowing for the relatively high temporal resolution analysis of biochemical changes associated with aerobic  $\text{CH}_4$  oxidation. The MIS was developed to house large mesocosm samples in a temperature-controlled and clean manner that did not allow gases to diffuse between the sample and the outside environment over the time frame of this experiment. The MIS contains custom 15-L sample bags that were tested for their cleanliness (i.e., no leaching of trace metals and nutrients) and gas impermeability over time (Chan et al., 2016). They were determined to be a better alternative than borosilicate glass as sample containers for these experiments because the bag material does not leach trace metals, is impermeable to gas exchange, and is of sufficient strength to house sample volumes  $>10$  L. Additionally, since the bags are flexible, aliquots can be periodically removed without contaminating the mesocosm by introducing a headspace for displacement. Since the DWH  $\text{CH}_4$  oxidation event occurred over

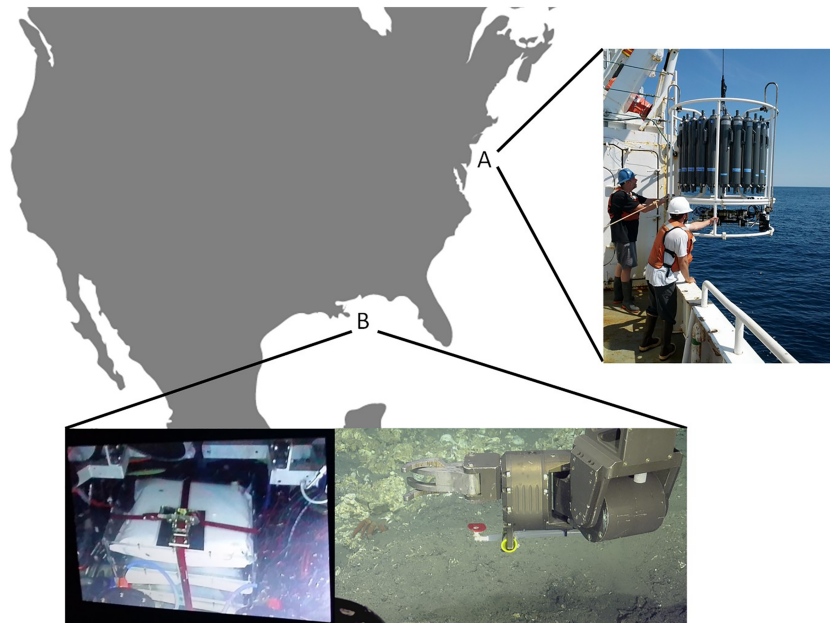


**Figure 2.** Study locations (a) Hudson Canyon and (b) a gas seep atop Woolsey Mound (also known as Sleeping Dragon) which is part of lease block MC118 in the northern Gulf of Mexico. Seawater samples in Hudson Canyon were collected with Niskin bottles cleaned for trace metal analysis and were used to sample waters that were both directly impacted and not directly impacted by CH<sub>4</sub> seepage. Water from MC118 was collected via ROV in locations visibly impacted by seafloor bubble emissions. On the left are the Mesocosm Incubation System (MIS) cartridges mounted to the chassis of ROV *Hercules*. On the right is the Suspended-Particle Rosette (SUPR) sampler inlet mounted to the starboard manipulator of ROV *Hercules* and methane bubbling upward from the seep site. A bubble-deflecting shield (red disk) was attached to the inlet of the SUPR sampler to collect seawater without collecting gas bubbles.

approximately 80 days, mesocosm incubations were designed to contain enough seawater to provide the necessary aliquots for analysis over that same time. To protect the bags from physical harm and provide a storage solution inside the incubator, the bags were housed in custom-made polycarbonate protective cartridges. In addition, the cartridges provide an easier way to carry the bags during sampling. Once the mesocosms were collected, the DGAS and MIS were connected to analyze the mesocosms based on set intervals, thus allowing near-real-time dissolved gas concentration and stable isotope measurements (Chan et al., 2016). The dissolved gas concentrations of CH<sub>4</sub>, O<sub>2</sub>, and CO<sub>2</sub> were measured every few seconds during each mesocosm analysis, and the individual measurements were averaged over a 2-min

**Table 1**  
*Hudson Canyon and Sleeping Dragon (MC118) Characteristics*

Site	Hudson Canyon	Sleeping Dragon (MC118)
Approximate coordinates	39°33'N, 72°24'W	28°51'N, 88°29.5'W
Topography	Semi-enclosed	Open
Sampling depths (m)	482–515	794, 888
Bottom temperature (°C)	5.25°–6.24°	5.31°–8.79°
Sampling dates	10 July 2014	13–17 April 2015
Sampling method	Niskin bottles	ROV (SUPR sampler)
Presence of oil	No	Yes
Salinity (ppt)	35.01–35.05	34.91–35.04
In situ dissolved oxygen concentration range (μM)	201–232	141–198
In situ CH <sub>4</sub> concentration range (nM)	2.94–78.8	51,000–221,000
Additional CH <sub>4</sub> added for incubation	Yes	No

window. After analysis of the data, it was determined that the DO analyzer manifold malfunctioned during the HC mesocosm incubations, resulting in the DO data from this experiment being sporadically unusable. For this reason, none of the DO data for HC was considered in the biogeochemical analyses. The DO analyzer manifold was redesigned before the MC118 experiments, resulting in usable DO data.

## 2.2. Mesocosm Collection

HC mesocosm experiments were initiated aboard the R/V *Endeavor* from 7–12 July 2014. Seawater was collected using trace metal cleaned Niskin bottles with external springs mounted to a CTD rosette (Figure 2; Shiller et al., 2017). Once the samples were back on the ship's deck, two 10-L Niskin bottles were connected to a MIS cartridge to fill with 15 L of seawater. The bags were acid cleaned, rinsed with distilled water, and rinsed with the sample seawater before filling to 15 L with seawater. Water samples were collected from inside the seep field (39°32.705'N, 72°24.259'W) and from outside HC in waters not directly influenced by CH<sub>4</sub> seeps (39°17.236'N, 72°12.080'W). Due to the spatial variance of the seafloor seeps, the initial CH<sub>4</sub> concentrations ranged from 2.94 to 78.8 nM. Therefore, a measured amount (150 ± 1.5 mL) of isotopically standardized CH<sub>4</sub> ( $\delta^{13}\text{C-CH}_4 = -20\text{‰}$ ; Kessler & Reeburgh, 2005) was systemically added to each sample using a mass flow controller and gas filter apparatus to increase dissolved CH<sub>4</sub> concentrations to approximately 300  $\mu\text{M}$  CH<sub>4</sub>. These samples were allowed 24 hr to mix and equilibrate inside the MIS before the headspace was removed prior to long-term incubation.

The MC118 mesocosms in the Gulf of Mexico were collected 12–17 April 2015 aboard the E/V *Nautilus* located at 28°51.129'N, 88°29.51'W directly from seeps at the seafloor between 794- and 888-m depth (Table 1 and Figure 2). This experiment was carried out using the Suspended-Particle Rosette (SUPR) sampler (Breier et al., 2009) mounted to the Remotely Operated Vehicle (ROV) *Hercules*. The SUPR sampler is an in situ seawater pumping system and was developed to sample dynamic, high gradient, and ocean geochemical features at areas such as seep sites. The inlet attached to the ROV arm pumps the seawater into bottles mounted to the SUPR sampler chassis. However, for this study, the system was adapted to pump directly into three of the MIS cartridges mounted to the ROV chassis, which improved the sampling precision substantially (Figure 2). Since samples were taken directly at the seafloor from waters visibly impacted by CH<sub>4</sub> bubbles, the natural dissolved CH<sub>4</sub> concentrations were high (51 to 221  $\mu\text{M}$ ); thus, it was not necessary to add additional CH<sub>4</sub> to these mesocosms. This simplified the procedure to incubate the MC118 mesocosms as there was no added headspace equilibration time, in contrast to the HC samples.

## 2.3. Dissolved Gas Concentration Calculations

The dissolved concentrations of CH<sub>4</sub> measured with the DGAS system give units of ppm (Chan et al., 2016), and it was preferred to convert this into units of  $\mu\text{mol}$  of CH<sub>4</sub> L<sup>-1</sup>. Two independent methods were used to convert the measured ppm concentrations into the molar concentrations of dissolved CH<sub>4</sub>. The first method prepared dissolved CH<sub>4</sub> standards by filling mesocosm incubation bags with sterile water containing known concentrations of dissolved CH<sub>4</sub>. These CH<sub>4</sub> standards were also stored in the MIS and analyzed with the DGAS system during the mesocosm experiments at sea. Standard calibration curves were determined for each experiment and were used to convert measured ppm units into units of  $\mu\text{mol}$  of CH<sub>4</sub> L<sup>-1</sup>. A second independent technique used the solubility of CH<sub>4</sub> (Wiesenburg & Guinasso, 1979) along with the known volumes of the liquid aliquot and the gaseous headspace being analyzed with the DGAS system to convert the measured ppm concentrations into units of  $\mu\text{mol}$  of CH<sub>4</sub> L<sup>-1</sup>. Both techniques produced similar results. The measured CO<sub>2</sub> concentration values were converted from ppm to  $\mu\text{mol}$  of CO<sub>2</sub> L<sup>-1</sup> following the second technique, but by incorporating the solubility for CO<sub>2</sub> at a salinity of 35 and 5 °C (53350  $\mu\text{M atm}^{-1}$ ; Weiss, 1974).

## 2.4. Microbial Community Analyses

Samples for DNA analysis were collected by removing 1-L aliquots from the mesocosm experiments at several time intervals and filtering them through 0.22- $\mu\text{m}$  Sterivex filters (Millipore). The filters were stored at -80 °C until analysis. DNA was extracted with the FastDNA SPIN Kit for Soil (MP Biomedicals). DNA was quantified with a Qubit 2.0 fluorometer (Life Technologies) and the Qubit dsDNA HS Assay Kit (Thermo Fisher Scientific). Amplification and sequencing of the V4 region of the 16S rRNA gene was done by Seqmatic with the Illumina MiSeq platform (2 × 250 bp), following the protocol described by Caporaso

et al. (2011). Sequence analysis was conducted with Mothur version 1.36.0 as described in the MiSeq SOP (Kozich et al., 2013), except that the SILVA (version 123) reference taxonomy was used for classification. This resulted in an average of 149,373 reads per sample. Sequences are available in the Sequence Read Archive under BioProject number PRJNA311933.

Aliquots were taken to detect bacterial cell abundance at various time points throughout both HC and MC118 mesocosms and were enumerated using flow cytometry following the protocol of Wear et al. (2015). Samples were collected in sterile cryovials, preserved with 0.2% final concentration of paraformaldehyde (Electron Microscopy Sciences, Hatfield, PA), flash frozen in liquid nitrogen, and stored frozen until analysis. Bacteria were stained with SYBR Green I (Molecular Probes) and enumerated with a BD LSRII flow cytometer (Becton Dickinson, San Jose, CA) with an autosampler attachment. Measurement of bacterial abundances for the HC samples was not successful due to technical failure with the flow cytometer after the preserved samples had already been thawed. However, the MC118 samples were analyzed successfully.

### 2.5. Macronutrient and Trace Metal Analyses

For each macronutrient analysis, 20 mL of seawater were removed from the mesocosm and passed through a 33-mm-diameter syringe filter with a 0.45- $\mu\text{m}$ -pore-size PVDF membrane (EMD Millipore) and stored frozen in HDPE scintillation vials until analysis. A Lachat Instruments QuikChem 8500 Series 2 Automated Ion Analyzer (Hach) was used by the UCSB Marine Science Institute Analytical Laboratory to obtain nutrient concentrations. Detection limits for nitrate + nitrite ( $\text{NO}_3^- + \text{NO}_2^-$ ), ortho-phosphate ( $\text{PO}_4^{3-}$ ), and ammonium ( $\text{NH}_4^+$ ) are 0.20, 0.10, and 0.10  $\mu\text{M}$ , respectively.

Water samples were isolated at interspersed time intervals to quantify the concentration of trace metals in the incubations. The specific trace metals targeted were Mn, Fe, Cu, Zn, Mo, La, Ce, Pr, Nd, Sm, and Eu. For analysis of dissolved trace elements, 7 mL of sample was spiked with a mixture of isotopically enriched Fe-57, Cu-65, Zn-68, Nd-145, Sm-149, and Eu-153 (Oak Ridge National Labs). Samples were then extracted/preconcentrated using a SeaFAST system (Elemental Scientific, Inc.) operated in off-line mode. A similar online SeaFAST extraction procedure is described by Hathorne et al. (2012). The extracted samples were subsequently analyzed using a Thermo-Fisher high-resolution ICP-MS (Element XR) with an Apex-FAST high-efficiency sample introduction system including a Spiro desolvator (Elemental Scientific, Inc.). The enriched isotope spikes allowed for isotope dilution quantification of the spiked elements and also served to provide counts/sec calibration factors for elements that were not spiked with enriched isotopes (Mn, Mo, La, Ce, and Pr). This calibration was also examined with a standard made in dilute nitric acid. Precision and recovery were checked by analysis of a large-volume composite North Atlantic surface seawater sample. Spiked (with a natural isotopic abundance elemental spike) and unspiked aliquots of this sample were analyzed twice in each analytical run. A Ba standard was also run to check for  $\text{BaO}^+$  interference on several isotopes and Ba in the extracted samples was also monitored. Due to the extraction resin in the SeaFAST system (Nobias PA-1) discriminating against Ba, in addition to the reduction of the  $\text{BaO}^+$  interference by the desolvation system,  $\text{BaO}^+$  was less than 0.1% of the counts in Eu-151 and Eu-153. A detailed description of the methods can be found in Shiller et al. (2017) and Ho et al. (2018). Detection limits were typically <1% of the concentrations reported here except for Ce and Eu, where detection limits were <5% of the reported concentrations. Precision (1  $\sigma$ ) was typically  $\pm 2\%$  and recoveries were typically  $102 \pm 3\%$ .

All data and descriptions of the analyses from these experiments are available through the Gulf of Mexico Research Initiative Information & Data Cooperative (GRIIDC; Kessler & Chan, 2017).

## 3. Results

### 3.1. Chemical Kinetics for Aerobic $\text{CH}_4$ Oxidation

Each incubation was monitored for unambiguous indications of aerobic  $\text{CH}_4$  oxidation by assessing changes in dissolved gas concentrations, isotope composition, microbial community composition, cell densities, and micronutrients and macronutrients, and this information was used to determine the beginning and ending of more rapid  $\text{CH}_4$  oxidation. While all experiments appeared to support microbial growth based on the microbial community composition and changes in cell density, partial blockages in some of the 1/8" tubing used to remove water from the MIS for chemical analysis caused variable results in several specific mesocosms. (To avoid this potential complication, future experiments are advised to insulate the 1/8" tubing



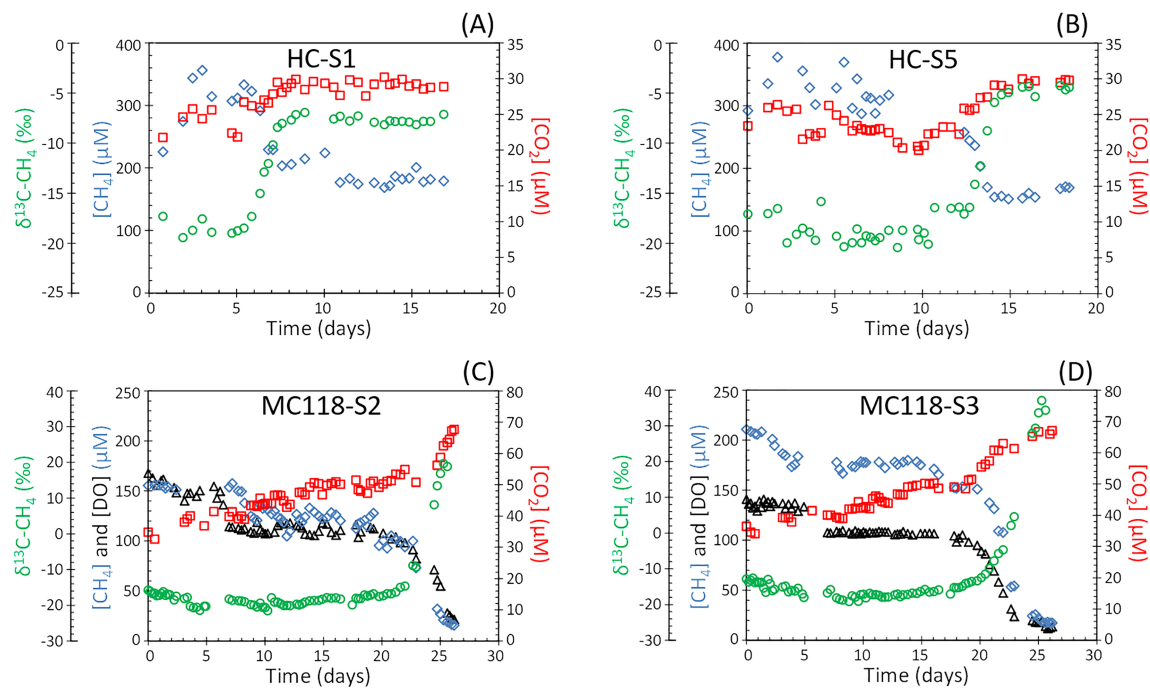


**Figure 3.** Dissolved concentrations of CH<sub>4</sub> (blue diamonds), CO<sub>2</sub> (red squares), and DO (black triangles), as well as δ<sup>13</sup>C-CH<sub>4</sub> (green circles) over the course of the incubations. (a) HC-S1 (on seep), (b) HC-S5 (off seep), (c) MC118-S2 (on seep), and (d) MC118-S3 (on seep). All data in these figures are available through the Gulf of Mexico Research Initiative Information & Data Cooperative (GRIIDC; Kessler & Chan, 2017).

when working at temperatures approaching 0 °C.) Considered here are the experiments that did not experience such analytical variabilities. Six of the 10 mesocosms with waters collected inside and adjacent to HC displayed clear biogeochemical signs of CH<sub>4</sub> oxidation (Figures 3a, 3b, and S1). Four of the 10 mesocosms collected with waters at MC118 displayed clear characteristics of CH<sub>4</sub> oxidation (Figures 3c, 3d, S3, and S4).

### 3.1.1. Time to Onset of Rapid CH<sub>4</sub> Oxidation

For the Hudson Canyon experiments, seawater was collected from waters impacted by known CH<sub>4</sub> seeps as well as waters outside of Hudson Canyon, not directly impacted by seeps. All samples were incubated at the same near in situ temperature (6 °C) to determine whether the presence of natural CH<sub>4</sub> seepage influenced methanotrophy. The mesocosms collected at the seep site (samples HC-S1 to -S2) initiated CH<sub>4</sub> oxidation approximately one week faster than the off-seep mesocosms (samples HC-S3 to -S6; Figures 3a, 3b, and S1

**Table 2**  
The Characteristics for Chemical Kinetics Determined in Hudson Canyon (HC) and MC118

Sample	Location	Lag time (day)	Duration (day)	DO:CH <sub>4</sub> (molar ratio)	k (day <sup>-1</sup> )
HC-S1	On seep	5.42	2.17	ND	0.25 ± 0.03
HC-S2	On seep	5.43	1.9	ND	0.18 ± 0.04
Ave and standard deviation	On seep	5.43 ± 0.01	2.0 ± 0.2		0.22 ± 0.05
HC-S3	Off seep	14.09	4.05	ND	0.054 ± 0.004
HC-S4	Off seep	12.64	3.05	ND	0.12 ± 0.01
HC-S5	Off seep	12.37	2.53	ND	0.24 ± 0.03
HC-S6	Off seep	8.85	6.34	ND	0.061 ± 0.003
Ave and standard deviation	Off seep	12 ± 2	4 ± 2		0.12 ± 0.09
MC118-S1	On seep	9.60	6.06	0.77	0.107 ± 0.005
MC118-S2	On seep	19.28	5.99	0.81	0.26 ± 0.04
MC118-S3	On seep	18.49	6.78	0.60	0.36 ± 0.04
MC118-S4	On seep	9.82	11.04	0.59	0.20 ± 0.02
Ave and standard deviation	On seep	14 ± 5	7.5 ± 2.4	0.7 ± 0.1	0.2 ± 0.1

*Note.* The units for lag time and duration are days, DO:CH<sub>4</sub> is unitless (μM/μM), and first-order oxidation rate constants (k) is day<sup>-1</sup>.

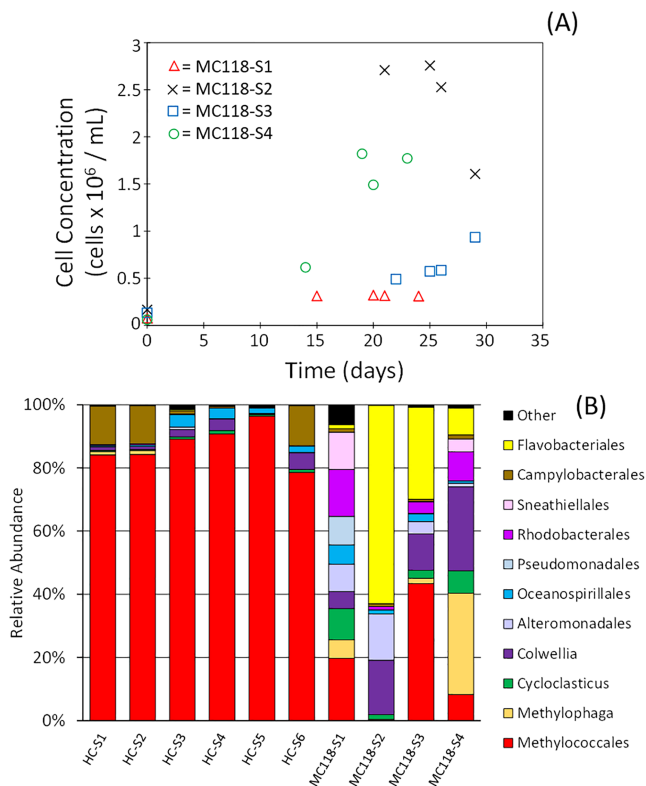


**Figure 4.** (a) Bacterial abundance across MC118 mesocosm samples. All samples exhibited cellular increases throughout the mesocosm incubations. Red triangles = MC118-S1, black cross = MC118-S2, blue squares = MC118-S3, and green circles = MC118-S4. (b) Microbial community compositions (%) from HC and MC118. Data displayed were collected at the end of each mesocosm.

congruent with the Kessler et al. (2011) model and the Crespo-Medina et al. (2014) data from the DWH incident (Figure 1). The HC mesocosms exhibited the highest first-order oxidation rate constant from HC-S1 at  $0.25 \pm 0.03 \text{ day}^{-1}$  and the lowest from HC-S3 at  $0.054 \pm 0.004 \text{ day}^{-1}$ , with an on-seep average of  $0.22 \pm 0.05 \text{ day}^{-1}$  and an off-seep average of  $0.12 \pm 0.09 \text{ day}^{-1}$ . The highest first-order oxidation rate constant at MC118 was MC118-S3 at  $0.36 \pm 0.04 \text{ day}^{-1}$ , the lowest was MC118-S1 at  $0.107 \pm 0.005 \text{ day}^{-1}$ , and the average was  $0.2 \pm 0.1 \text{ day}^{-1}$  (Table 2). These rate constants are within the range, but occasionally slightly higher than the rate constants predicted in Kessler et al. (2011;  $0.0001\text{--}0.200 \text{ day}^{-1}$ ) and measured in Crespo-Medina et al. (2014;  $0.0001\text{--}0.425 \text{ day}^{-1}$ ) for  $\text{CH}_4$  oxidation in the deepwater plumes during the DWH blowout (Figure 1). Since the rate constants reported here were determined in a closed-system without dilution of cells and substrates, it is not surprising that the rate constants are elevated compared to those determined in the natural environment where such dilution was experienced (Crespo-Medina et al., 2014). It is also interesting to note the differences between the observations here and what was assumed in the Kessler et al. (2011) model. The Kessler et al. (2011) model assumed that the rate constants would increase at the start of rapid  $\text{CH}_4$  oxidation and decrease as  $\text{CH}_4$  concentrations decreased and this process became reactant limited. However, the empirical data here suggest that the rate constants remain invariant for the remainder of this experiment after the onset of rapid  $\text{CH}_4$  oxidation (Table 2, see “Duration” column for length of time it was invariant), more similar to the rate constant data reported in Crespo-Medina et al. (2014) for the deepwater plumes (Figure 1).

### 3.1.3. Microbial Community

The goal of the biological analyses was to determine what microbial community was supporting  $\text{CH}_4$  oxidation and the extent to which this microbial population bloomed during  $\text{CH}_4$  oxidation. To accomplish this goal, changes in bacterial abundance were quantified (Figure 4a) and the 16S rRNA gene was sequenced

and Table 2). After the onset of rapid methane oxidation, the on-seep mesocosms depleted their nutrient and trace metal resources and thus completed oxidation in two days on average, whereas the off-seep mesocosms completed oxidation in four days on average (Figure S1 and Table 2). The results from the Atlantic margin suggest that  $\text{CH}_4$  oxidation can occur in waters with and without the direct influence of  $\text{CH}_4$  seeps. However, seeps in a partially enclosed environment such as a submarine canyon, likely keep the waters with a higher starting density of methanotrophic bacteria and thus “primed” for a faster methanotrophic response. This finding appears consistent with previous studies (Leonte et al., 2017; Weinstein et al., 2016).

At MC118, since the mesocosms were collected directly from the seep site with an ROV, the waters all contained naturally high concentrations of  $\text{CH}_4$  leading us to the hypothesis that  $\text{CH}_4$  oxidation would occur more rapidly than in Hudson Canyon. However, this was not the case, with the mesocosms taking 14 days on average to initiate rapid  $\text{CH}_4$  oxidation and an additional 7.5 days on average until oxidation became limited by a reactant (Figures 3c, 3d, S3, and S4 and Table 2). We suspect that the less topographically restricted MC118 seep field results in more rapid replacement of the ambient waters likely leading to a lower resident methanotrophic population than HC.

### 3.1.2. Rate Constants for $\text{CH}_4$ Oxidation

For the mesocosms that displayed  $\text{CH}_4$  oxidation, we determined whether  $\text{CH}_4$  oxidation after the onset of rapid  $\text{CH}_4$  oxidation followed zeroth-, first-, or second-order kinetic rate laws as well as the rate constants for the resulting rate law throughout this rapid oxidation process. The procedures used for determining the rate constants can be found in the supporting online information. While the concentration data alone did not clearly distinguish between these reaction orders, the isotope data more clearly indicated that methane consumption followed first-order kinetics (see below and the companion paper). This conclusion is

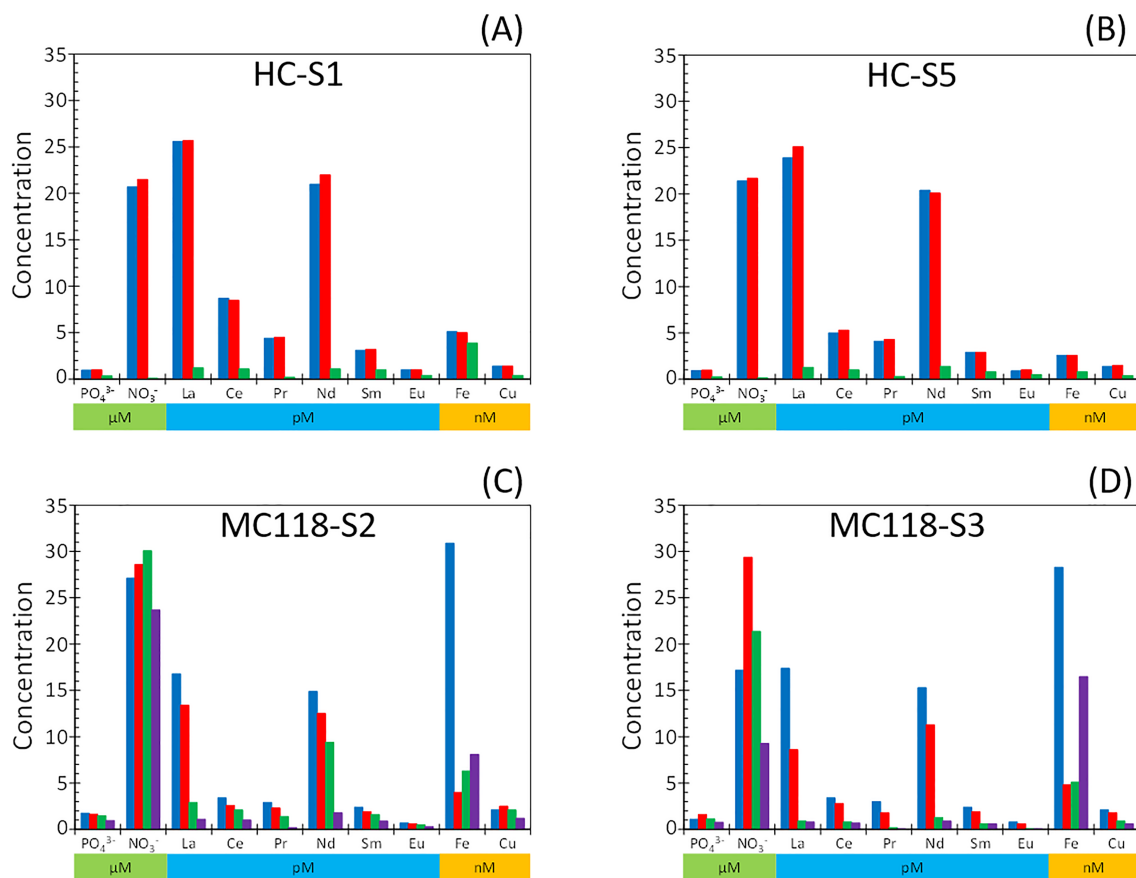


**Figure 5.** Nutrient and trace metal results from HC and MC118 mesocosms. (a and b) Blue = time 0 day sample collected directly from the Niskin bottle, red = time 0 day sample collected from the mesocosm bag, and green = samples collected from the mesocosm bag at the end of the incubation, time = 19–21 days. The two  $t = 0$  day samples (blue and red) were analyzed to determine if there was any nutrient or trace metal contamination associated with the transfer to the sample bags. (c and d) Since the MC118 seawater samples were collected directly into the incubation bags, all samples were collected from the bags at different times. Blue = 0 day, red = 17–22 days, green = 25 days, violet = 29 days.

to determine the composition of the microbial communities (Figure 4b). Comparing these microbial analyses can suggest a growing population of specific microbial communities identified by the 16S rRNA analyses. For both the HC and MC118 mesocosms, the overall results suggest a growing population of organisms previously linked to CH<sub>4</sub> oxidation over the course of these incubations. All incubations began with an extended lag period typical for required adaptation and growth of the bacteria.

Bacterial abundance measurements for the HC mesocosms were not measured because of the aforementioned technical failure. However, the DNA measurements and the change in respiration rate suggest such a bloom occurred. The DNA samples from the beginning of the incubation had low DNA yields and were difficult to amplify. This contrasts with the DNA samples from the end of the incubation, where the sequencing of the 16S rRNA gene was successful consistent with higher cellular abundances (Table S2). Methylococcales, which have been previously linked to aerobic CH<sub>4</sub> oxidation (e.g., Redmond et al., 2010; Redmond & Valentine, 2012), constituted 78–97% of 16S rRNA genes sequenced in HC (Figure 4b). The dominance of organisms previously linked to CH<sub>4</sub> oxidation in the HC incubations is likely due to CH<sub>4</sub> being the primary substrate in these mesocosms.

The MC118 bacterial abundance indicates cellular growth across all mesocosms (Figure 4a). Similar to the HC experiments, Methylococcales was also present in MC118 experiments, and when considered alongside cell abundance, indicates a growing population of organisms previously linked to CH<sub>4</sub> oxidation. While Methylococcales constituted a lower percentage of the microbial community in the MC118 mesocosms compared to the HC mesocosms, the MC118 mesocosms were collected directly from a seep that also emits other oil and gaseous hydrocarbons. Thus, this smaller fraction of putative methanotrophs is presumably due to

concurrent blooms of other hydrocarbon degrading species (Figure 4; Reddy et al., 2012; Redmond & Valentine, 2012; Redmond et al., 2010). Redmond and Valentine et al. (2012) observed very similar communities in samples collected in this region of the Gulf of Mexico during the DWH oil spill. Overall, in addition to a growing population of organisms previously linked to CH<sub>4</sub> oxidation, these data also suggest that for both HC and MC118, a significant amount of the methanotrophic biomass remained when the mesocosms were terminated that had not been fully remineralized to CO<sub>2</sub>.

### 3.2. Amounts of Substrates Required to Oxidize a Quantity of CH<sub>4</sub>

#### 3.2.1. General Dissolved Gas Concentration Changes

Of the six mesocosms in HC that exhibited CH<sub>4</sub> oxidation, an average of  $98 \pm 24$  μM (standard deviation of natural variability between mesocosms) of the CH<sub>4</sub> available in each sample was consumed. The average increase in dissolved CO<sub>2</sub> concentration was  $4.7 \pm 1.4$  μM (Table S1).

Since the initial concentration of dissolved CH<sub>4</sub> was variable in the samples collected at MC118 and different from the HC samples, differences in the absolute concentration changes were also observed. Of the four mesocosms that displayed CH<sub>4</sub> oxidation, dissolved CH<sub>4</sub> concentration showed an average decrease of  $83 \pm 58$  μM over the course of the mesocosm experiments. Where there was CH<sub>4</sub> oxidation, there were concomitant decreases in DO and increases in dissolved CO<sub>2</sub> concentrations (Figures 3c, 3d, S3, and S4). On average, the DO decreased by  $56 \pm 38$  μM during the incubations from MC118. The average ratio of DO:CH<sub>4</sub> removed in MC118 was  $0.7 \pm 0.1$  (Table 2). Dissolved CO<sub>2</sub> being produced further supports the occurrence of CH<sub>4</sub> oxidation, with an average increase of  $18 \pm 4$  μM throughout the MC118 experiments (Table S1).

#### 3.2.2. General Nutrient and Trace Metal Concentration Changes

The starting concentrations of nutrients and Fe in the HC mesocosms were lower than for the MC118 mesocosms. The proximity to the sediment interface and intermittent resuspension of sediment by violent bursts of CH<sub>4</sub> (EV Nautilus, 2015) likely caused these higher concentrations found at MC118 (D'souza et al., 2016), which is especially apparent in the Fe concentrations (Figures 5 and S6–S9). For example, the average starting Fe concentration in the HC was  $3.2 \pm 1.3$  nM whereas MC118 displayed average values of  $21 \pm 10$  nM (Figure 5). Throughout the HC mesocosm incubations, both PO<sub>4</sub><sup>3-</sup> and NO<sub>3</sub><sup>-</sup> had high utilization (Figures 5 and S6) and cietrace metal results from H CH<sub>4</sub> oxidation. In contrast, the MC118 incubations did not display a decrease in PO<sub>4</sub><sup>3-</sup> and NO<sub>3</sub><sup>-</sup> to the point of limitation (Figures 5 and S7), but it is worth noting that the starting concentrations of CH<sub>4</sub> were less in MC118 than in HC (Table S1).

The trace metal analysis demonstrated pronounced depletions during all mesocosm incubations. The methanol dehydrogenase (MDH) enzyme that catalyzes the second step in CH<sub>4</sub> oxidation is often Ca (II)-dependent (MxaF type) and methane monooxygenase incorporates Cu and Fe (Fox et al., 1988; Murrell et al., 2000; Ross et al., 2019). However, recent discoveries with methano- and methyl-trophic bacteria have suggested that light rare earth elements (LREE), specifically La, Ce, Pr, Nd, and Sm, may play a significant role in the oxidation of methane and methanol (Huang et al., 2018; Picone & Op den Camp, 2019; Pol et al., 2014). Lanthanum (La), one of the lanthanides identified in CH<sub>4</sub> oxidation studies (Pol et al., 2014; Shiller et al., 2017), had an average decrease of  $23 \pm 2$  pM in the HC mesocosms and  $15 \pm 2$  pM in the MC118 mesocosms (Figures 5, S8, and S9). While La displayed the highest percentage removed, other LREEs that were removed during the microbial bloom were cerium (Ce), praseodymium (Pr), neodymium (Nd), samarium (Sm), and europium (Eu); these additional LREEs exhibited significant decreases, possibly limiting CH<sub>4</sub> oxidation (Kessler & Chan, 2017). Slightly lower depletions in LREEs at MC118 were observed, which we suspect is due to the lower starting concentrations of CH<sub>4</sub> than in the HC mesocosms. Cu and Fe decreases were also notable at 0.8 to 1.3 and 0.7 to 1.8 nM, respectively, in HC mesocosms (Figures 5 and S8). MC118 mesocosms showed larger Fe decreases than HC mesocosms at 6.9 to 22.8 nM, perhaps due to the oxidation of non-CH<sub>4</sub> hydrocarbons (Figures 5 and S9).

## 4. Discussion

### 4.1. Mesocosm Stoichiometric Ratios for Aerobic CH<sub>4</sub> Oxidation

An elemental stoichiometric ratio for CH<sub>4</sub> oxidation would be useful for predicting the sufficiency of the environment to supply essential nutrients and trace metals to enable the oxidation of CH<sub>4</sub>. For the most

**Table 3**  
Mesocosm Stoichiometric Ratios for Aerobic Methane Oxidation

	CH <sub>4</sub>		DO		NO <sub>3</sub> <sup>-</sup>		PO <sub>4</sub> <sup>3-</sup>	
HC	144 ± 45		ND		30 ± 5		1	
MC118	210 ± 190		140 ± 110		19 ± 11		1	
Average	148 ± 44		140 ± 110		28 ± 5		1	

	CH <sub>4</sub> (×10 <sup>6</sup> )	DO (×10 <sup>6</sup> )	La	Ce	Pr	Nd	Sm	Eu	Fe	Cu
HC	4.4 ± 1.3	ND	1	0.22 ± 0.07	0.17 ± 0.01	0.78 ± 0.08	0.07 ± 0.02	0.02 ± 0.01	57 ± 21	44 ± 7
MC118	5.3 ± 3.3	3.6 ± 2.2	1	0.26 ± 0.13	0.16 ± 0.03	0.71 ± 0.28	0.08 ± 0.04	0.03 ± 0.01	850 ± 420	40 ± 40
Average	4.5 ± 1.2	3.6 ± 2.2	1	0.23 ± 0.06	0.17 ± 0.01	0.77 ± 0.08	0.07 ± 0.02	0.03 ± 0.01	60 ± 20	44 ± 7

Note. The averages reported, and their associated standard deviations, are weighted to the uncertainties of the HC and MC118 values.

accurate determination of a stoichiometric ratio for CH<sub>4</sub> oxidation, the analysis of a pure culture of aerobic methanotrophs would be required. However, using pure culture ratios to predict CH<sub>4</sub> oxidation based on measured concentrations of nutrients or trace metals in the natural environment would be challenging; competing processes in the natural environment, such as denitrification and the oxidation of nonmethane hydrocarbons, could also influence changes in these compounds and confuse predictions of the extent of CH<sub>4</sub> oxidation. Furthermore, cultivation tends to favor rapid-growth phenotypes that may lack environmental relevance. Thus, our approach was to use mesocosm incubations so that uncertainties due to these competing processes and potential cultivation bias would be included in the final results. So, while our mesocosm approach likely incurs more uncertainty for a stoichiometric ratio specific to CH<sub>4</sub> oxidation, the intent was that it would provide a reasonable range of possible concentration changes to be observed during an aerobic CH<sub>4</sub> oxidation event in the natural environment. Since concentration changes in DO, CH<sub>4</sub>, nutrients, and trace metals were determined throughout these incubations, two different ratios were established, one for CH<sub>4</sub>-to-nutrients and another for CH<sub>4</sub>-to-trace metals (Table 3).

The CH<sub>4</sub>:N:P ratios for HC were similar for both the on- and off-seep sampling locations, with an average ratio of (144 ± 45):(30 ± 5):(1). The CH<sub>4</sub>:DO:N:P ratio for MC118 mesocosms was (210 ± 190):(140 ± 110):(19 ± 11):(1). The variability in the MC118 nutrient ratio is likely caused by variable competition for the available nutrients coupled with the oxidation of nonmethane hydrocarbons. Due to the relatively elevated uncertainty in the MC118 ratio, the nutrient ratios are statistically similar between HC and MC118. Similar conclusions are reached when investigating the ratio of CH<sub>4</sub>:DO:La:Ce:Pr:Nd:Sm:Eu:Fe:Cu; in that, the results from HC were statistically similar to MC118, given the variability observed in these environments (Table 3). Increased uncertainty in the MC118 trace metal stoichiometric ratio for CH<sub>4</sub> oxidation was most apparent in Fe, Cu, and Nd, likely caused by different amounts of oxidation of non-CH<sub>4</sub> hydrocarbons. It is interesting to note that Pol et al. (2014) showed that La-Ce-Pr-Nd are all utilized similarly, and that the utilization decreased with higher MW elements. However, while our stoichiometric ratios for La:Nd are in roughly equal proportions, our stoichiometric ratios for La:Sm are significantly less than what might have been expected based the results of Pol et al. (2014) yet are likely related to the decreased utilization of heavier REEs (Picone & Op den Camp, 2019; Table 3).

Although the biogeochemical conditions are different at the sites investigated, the stoichiometric ratios from both the HC and MC118 mesocosms indicate that nutrients and trace metals were utilized in similar proportions (Table 3). Despite the MC118 incubations also involving the oxidation of non-CH<sub>4</sub> hydrocarbons (Figure 4), the similarity of results is likely caused by CH<sub>4</sub> being the dominant hydrocarbon available for oxidation at the beginning of each mesocosm. This further suggests that the stoichiometric ratios for aerobic CH<sub>4</sub> oxidation presented here can possibly be used to estimate CH<sub>4</sub> consumption at other oceanographic seep sites, even if concurrent (secondary) biochemical processes are occurring. Certainly, future studies investigating the chemical requirements for CH<sub>4</sub> oxidation should also consider monitoring other biochemical processes occurring concurrently such as the oxidation of higher-order hydrocarbons and nitrogen transformations (Voss et al., 2013), both of which likely occurred in these experiments. For example, the trace metal analyses reported here displayed changing Mo concentrations and the nutrient analyses

displayed increases in nitrite (Kessler & Chan, 2017), possibly related to nitrogen dynamics in these incubations (Bertine, 1972; Collier, 1985).

#### 4.2. Evaluating the Reaction Chain for Aerobic CH<sub>4</sub> Oxidation to Interpret the Observed DO:CH<sub>4</sub>

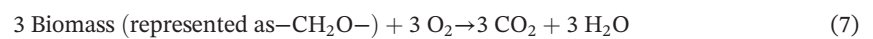
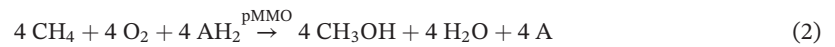
The overall reaction for aerobic CH<sub>4</sub> oxidation is generally described with equation (1), indicating that if one mole of CH<sub>4</sub> is fully oxidized to CO<sub>2</sub>, two moles of DO will be removed.



However, if CH<sub>4</sub> is not fully converted to CO<sub>2</sub>, for example, through the formation of biomass or intermediates, less than two moles of O<sub>2</sub> will be utilized. Only after the biomass/intermediates are mineralized to CO<sub>2</sub> will the full two moles of O<sub>2</sub> be removed. For each of the mesocosm experiments conducted in MC118, the DO:CH<sub>4</sub> ratio was less than two (Table 2), suggesting that the formation of biomass and intermediates was significant. Since both the cell count and 16S rRNA gene survey data also indicate that significant methanotrophic biomass formed during these incubations and was still present when these experiments were terminated (Figure 4), it is not surprising that less DO was removed than would have been expected for complete remineralization to CO<sub>2</sub>. What is surprising is that the average values for the DO:CH<sub>4</sub> ratios were slightly less than one (Table 2). While we cannot fully discredit that this slight deviation from unity is explained by an unidentified analytical error, we instead investigate the reaction mechanism of aerobic CH<sub>4</sub> oxidation to raise possible biochemical explanations.

Since aerobic CH<sub>4</sub> oxidation is a microbially mediated process, biological growth processes occur concurrently, utilizing a portion of the substrates to produce cellular organic matter. It has been well documented that CH<sub>4</sub> oxidation occurs through soluble and particulate CH<sub>4</sub> monooxygenase enzymes (sMMO and pMMO, respectively), and that most type I methanotrophs closely related to those identified in these mesocosms predominantly use the membrane-bound pMMO (Kalyuzhnaya et al., 2013; Murrell et al., 2000). While sMMO function is well documented, the exact mechanism of pMMO is not completely known with only predicted biochemical pathways (Kalyuzhnaya et al., 2013). The first step of the CH<sub>4</sub> oxidation process with pMMO has CH<sub>4</sub> being converted to methanol (CH<sub>3</sub>OH; equation (2)), requiring electron acceptors and donors (i.e., redox cofactors such as nicotinamide adenine dinucleotide (NAD) and pyrroloquinoline quinone (PQQ) represented simply in the equations here as A and AH<sub>2</sub>). Next, methanol is converted to formaldehyde (CH<sub>2</sub>O; equation (3)) via methanol dehydrogenase (MDH; Bédard & Knowles, 1989; Kalyuzhnaya et al., 2013). Following this step, there are three possible pathways for formaldehyde to be utilized by the cell: (1) assimilation into biomass via the ribulose monophosphate (RuMP) pathway (equation (4); Dalton & Leak, 1985; Kalyuzhnaya et al., 2013; Quayle & Ferenci, 1978), (2) further oxidation to CO<sub>2</sub> (equations (5) and (6); Bédard & Knowles, 1989; Kalyuzhnaya et al., 2013), or (3) assimilation into the serine pathway. Concerning pathway (2), the formaldehyde is converted to formate by formaldehyde dehydrogenase (FaLDH; equation (5); Bédard & Knowles, 1989). Formate is then converted to CO<sub>2</sub> via formate dehydrogenase (FDH; equation (6); Bédard & Knowles, 1989). Thus, CO<sub>2</sub> can be produced and measured in these mesocosms without first forming cellular biomass via the RuMP pathway. However, part of the formaldehyde is used to create biomass in pathway (1), and thus, the amount of carbon remaining as biomass must be considered.

To produce a balanced aerobic CH<sub>4</sub> oxidation reaction series, we hypothesize the following stoichiometry. Since three moles of formaldehyde are required for biomass assimilation via the RuMP pathway (Kalyuzhnaya et al., 2013) and one mole of formaldehyde is required for the oxidation to CO<sub>2</sub> via pathway (2), there needs to be a total of four moles of CH<sub>4</sub> and four moles of O<sub>2</sub> that begin this microbially mediated reaction. To balance the system of equations, the oxidization of the biomass that is created must be considered (equation (7)). In equation (7), biomass is more generally represented as a –CH<sub>2</sub>O– chain. Lastly, these reactions would not occur without electron transport within a biological system, and thus, an equation for a terminal electron acceptor/donor pair is needed. In an aerobic CH<sub>4</sub> oxidation environment, it is DO that serves as this electron acceptor with many electron transport chains, cytochromes, etc. that facilitate this process (equation (8)). The simplification of this system of equations results in the overall aerobic CH<sub>4</sub> oxidation equation (equation (1)).



Based on these hypothesized reactions, the DO:CH<sub>4</sub> ratio should not drop below 1:1. However, the MC118 incubations ended with an average DO:CH<sub>4</sub> of 0.7 ± 0.1. While synergies with other organisms can remove more CH<sub>4</sub> and provide more electron donors, such as anaerobic oxidation of CH<sub>4</sub> linked to denitrification identified near the sediment-water interface (Raghoebarsing et al., 2006; Waki et al., 2002) or aerobic methane oxidization coupled with nitrate reduction in hypoxic environments (Kits et al., 2015), our mesocosms did not have enough dissolved nitrate to account for the extra DO demand. For example, if we assume that nitrate provides oxygen to further oxidize CH<sub>4</sub>, the measured decrease in nitrate during the MC118 mesocosms is only sufficient in one of the four mesocosms to raise the DO:CH<sub>4</sub> to 1:1. A DO:CH<sub>4</sub> of less than 1:1 could also be explained if equation (2) did not produce water. In this hypothetical reaction mediated with pMMO, the DO:CH<sub>4</sub> in the initial step of aerobic CH<sub>4</sub> oxidation would only be 0.5:1. We note that this stoichiometry is consistent with the first step of the pMMO-catalyzed reaction cycle, but requires differences in the latter stages than assumed for pMMO in biochemical studies (Culpepper & Rosenzweig, 2012; Sirajuddin & Rosenzweig, 2015). While additional systematic experiments are required to confirm the true reaction mechanism and explain the occurrence of DO:CH<sub>4</sub> ratios <1, our data clearly indicate that two moles of DO is not an inherent requirement for the oxidation of one mole of CH<sub>4</sub>. Even though the goal of this study was not to determine cellular biochemical functions in methanotrophs, the hypothesized reaction mechanism produced from these experiments can serve as a starting point for future experiments.

### 4.3. Deepwater Horizon Implications

The information learned from the mesocosm incubations can be used to better understand the fate of CH<sub>4</sub> dissolved in the deep hydrocarbon intrusion layers during the DWH blowout in the Gulf of Mexico. First, the biogeochemical conditions at the start of the MC118 incubations were likely more similar to the conditions experienced during the DWH blowout than the samples from HC. The nutrient and trace metal concentrations in the MC118 mesocosm were similar to those experienced during the DWH (Joung & Shiller, 2013; Shiller & Joung, 2012) and there was likely competition between methanotrophs and other hydrocarbon oxidizers for available resources. The MC118 mesocosms showed that approximately 80% of the dissolved CH<sub>4</sub> was oxidized in approximately 19–25 days (Tables 2 and S1 and Figures 3, S3, and S4). Certainly, outside of these mesocosm incubation bags mixing in the deep Gulf of Mexico would influence these results since mixing would dilute CH<sub>4</sub> concentrations and methanotrophic cell density but would add fresh DO, nutrients, and trace metals into a parcel of CH<sub>4</sub>-laden water. Nonetheless, the results presented here display that a near-complete oxidation is possible even without added reactants from mixing. Second, the Kessler et al. (2011) model of DWH CH<sub>4</sub> oxidation (Figure 6) suggests that CH<sub>4</sub> oxidation rate constants averaged over the entire plume peaked approximately 20 days after the CH<sub>4</sub> source to the water column stopped. Perhaps coincidentally, the highest rate constant determined from the mesocosm experiments presented here for MC118 occurs approximately 20 days after the parcel of CH<sub>4</sub>-laden water was isolated (Figure 6). In addition, the magnitude of the oxidation rate constants determined here is in agreement with the model and previous measurements. Third, applying the stoichiometric ratio derived from the HC

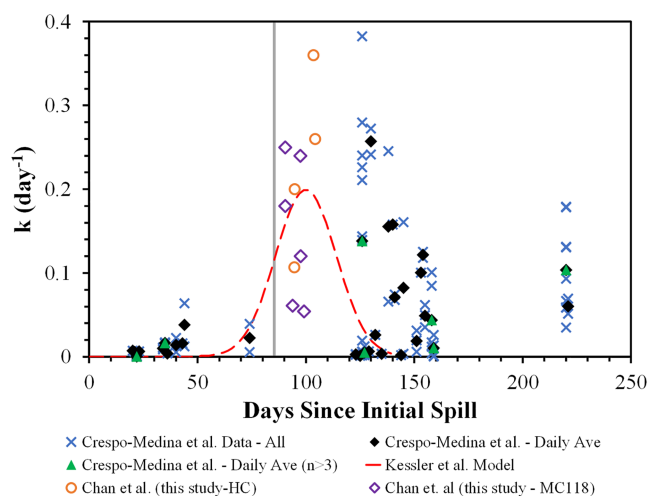


**Figure 6.** The first-order rate constants for aerobic CH<sub>4</sub> oxidation determined here from HC and MC118 superimposed on the DWH data presented in Figure 1. Violet diamonds = rate constants determined here from the HC experiments. Orange circles = rate constants determined here from the MC118 experiments. All other symbols are the same as indicated in Figure 1. The horizontal (i.e., time in days) position for the data determined here is the time until the start of rapid CH<sub>4</sub> oxidation plotted relative to the day the DWH blowout was stopped and no longer injecting CH<sub>4</sub> into Gulf of Mexico waters (vertical gray line).

$\times 10^{11}$  moles of CH<sub>4</sub>. Reddy et al. (2012) determined that  $6.23 \times 10^9$  moles of CH<sub>4</sub> were released during the DWH event which is <1% of the CH<sub>4</sub> oxidation potential of the impacted waters. This does not provide proof of the fate of CH<sub>4</sub> during this event; however, it does add further support to our previous contention that DWH CH<sub>4</sub> was fully oxidized in the deep intrusion layers and provides empirical biogeochemical data to characterize an entire oxidation event.

Finally, another result reported here relevant to the DWH blowout is the DO:CH<sub>4</sub> ratio. In MC118 mesocosms, the DO:CH<sub>4</sub> ratios suggest that a significant portion of the oxidized CH<sub>4</sub> is being converted to biomass and potentially intermediates (e.g., methanol) instead of fully to CO<sub>2</sub>. Du and Kessler (2012) estimated that  $60\% \pm 40\%$  of the deep intrusion layer hydrocarbon mass was oxidized based on complete conversion to CO<sub>2</sub>. However, if a significant portion of this CH<sub>4</sub>-C remained as biomass, the DO demand for CH<sub>4</sub> oxidation would have been less, and a near-complete removal of CH<sub>4</sub> could have been supported.

## 5. Conclusions

Mesocosm incubations of seawater collected in two seep fields, one in the North Atlantic Bight in and near Hudson Canyon and the other in the Gulf of Mexico, were used for the controlled study of biogeochemical changes during aerobic CH<sub>4</sub> oxidation. The analysis of dissolved gases (CH<sub>4</sub>, CO<sub>2</sub>, DO) in real-time and in high resolution permitted monitoring of each mesocosm experiment and provided the opportunity to analyze for other parameters such as microbial genetics, cell abundance, nutrients, and trace metals at critical times during this CH<sub>4</sub> oxidation process. This sampling frequency captured the different stages of these CH<sub>4</sub> oxidation events and was possible due to the controlled and isolated nature of the mesocosm incubations; conducting a similar study of a CH<sub>4</sub> perturbation in nature, such as the DWH blowout, would have been logistically challenging due to more heterogeneous and multivariate conditions occurring at-depth over an area of approximately 73,000 km<sup>2</sup> (Du & Kessler, 2012).

While the initial biogeochemical conditions at the seeps on the Atlantic Margin were different from those in the Gulf of Mexico, several similarities in the characteristics of CH<sub>4</sub> oxidation were observed. The stoichiometric ratio results for CH<sub>4</sub> oxidation were statistically similar between both environments despite greater natural variability in the Gulf of Mexico, likely due to the influence of non-CH<sub>4</sub> hydrocarbon oxidation

samples for CH<sub>4</sub> oxidation to Fe concentrations measured in waters during the DWH blowout (0.3–2.2 nmol/kg; Joung & Shiller, 2013) suggests that 23 to 170 μM of CH<sub>4</sub> could potentially be oxidized. Using the stoichiometric ratio derived from the MC118 mesocosms predicts that 2 to 14 μM CH<sub>4</sub> oxidation could be supported. Estimating CH<sub>4</sub> oxidation using decreases in La during the DWH blowout (Shiller et al., 2017) and applying the stoichiometric ratio from HC seeps, respectively, yields 18 to 53 μM of CH<sub>4</sub> oxidation that could be supported, while using the MC118 stoichiometric ratio suggests that 21 to 64 μM of CH<sub>4</sub> oxidation could be supported. The range of estimates for DWH CH<sub>4</sub> oxidation potential is due to the different concentrations of initial reactants in these experiments as well as resource competition with bacteria conducting other concurrent metabolisms. While CH<sub>4</sub> concentrations heterogeneous over the extent of the deep intrusion layers during the DWH incident, the capacity for DWH CH<sub>4</sub> to be oxidized, as predicted here with the mesocosm results, is greater than all but a handful of measurements of CH<sub>4</sub> concentration during and after conditions of active release from the well (Crespo-Medina et al., 2014; Joye et al., 2011; Kessler et al., 2011; Reddy et al., 2012; Valentine et al., 2010; Yvon-Lewis et al., 2011).

Also, if we scale the average concentration of CH<sub>4</sub> removed via oxidation in these mesocosm incubations ( $90 \pm 40$  μM) to the entire volume of the deepwater plume during the DWH incident (approximately  $7.3 \times 10^{15}$  L; Du & Kessler, 2012), we can estimate the total capacity for CH<sub>4</sub> oxidation during the DWH incident. This scaling exercise results in a value of  $7 \pm 3$



processes. Both the experiments presented here (Figure 3) and those from the DWH blowout (Figure 1) suggest that a significant lag phase precedes rapid CH<sub>4</sub> oxidation. In the semiconfined environment of Hudson Canyon, this lag time was approximately one week on average while it was approximately two weeks in more open ocean environments outside of Hudson Canyon and in the Gulf of Mexico. Following this lag time, our experiments show that the CH<sub>4</sub> oxidation rate constants increased substantially and remained high even after the CH<sub>4</sub> concentration decreased significantly, a finding which appears congruent with measurements during and after the DWH blowout (Figure 1; Crespo-Medina et al., 2014; Rogener et al., 2018). Since CH<sub>4</sub> oxidation follows first-order kinetics, the persistence of elevated rate constants suggests that the remineralization of methanotrophic biomass may be slow and thus that CH<sub>4</sub> oxidation could start rapidly without a lag phase, or with an abbreviated lag phase, if CH<sub>4</sub> concentrations again rose, as modeled previously (Valentine et al., 2012). Thus, these data suggest that a natural environment may remain primed to oxidize future releases of CH<sub>4</sub>, although the extent and duration remains untested.

### Acknowledgments

This work was made possible by grants from the National Science Foundation (OCE-1318102 to J.D.K.) and the Gulf of Mexico Research Initiative through the GISR (to J.D.K.) and CONCORDE (to A.M.S.) consortia. Support for D.L.V. and E.C.A. also came primarily from OCE-1318102, but secondary support was provided by the NSF (OCE-1333162 and OCE-1756947). Data are publicly available through the Gulf of Mexico Research Initiative Information & Data Cooperative (GRIIDC) at <https://data.gulfresearchinitiative.org/data/R1.x137.000:0019>. We thank the captain and crew of the R/V *Endeavor* and the E/V *Nautilus* as well as Bill Fanning and Nicole Raineault for their enthusiasm and support at sea. Finally, we would like to thank Patrick Crill, an anonymous reviewer, and the Editor for the constructive suggestions which helped to strengthen this manuscript.

### References

- Bédard, C., & Knowles, R. (1989). Physiology, biochemistry, and specific inhibitors of CH<sub>4</sub>, NH<sub>4</sub><sup>+</sup>, and CO oxidation by methanotrophs and nitrifiers. *Microbiological Reviews*, 53(1), 68–84.
- Bertine, K. K. (1972). The deposition of molybdenum in anoxic waters. *Marine Chemistry*, 1(1), 43–53. [https://doi.org/10.1016/0304-4203\(72\)90005-9](https://doi.org/10.1016/0304-4203(72)90005-9)
- Breier, J. A., Rauch, C. G., McCartney, K., Toner, B. M., Fakra, S. C., White, S. N., & German, C. R. (2009). A suspended-particle rosette multi-sampler for discrete biogeochemical sampling in low-particle-density waters. *Deep Sea Research Part I: Oceanographic Research Papers*, 56(9), 1579–1589. <https://doi.org/10.1016/j.dsr.2009.04.005>
- Camilli, R., Reddy, C. M., Yoerger, D. R., Van Mooy, B. A. S., Jakuba, M. V., Kinsey, J. C., et al. (2010). Tracking hydrocarbon plume transport and biodegradation at Deepwater Horizon. *Science*, 330(6001), 201–204. <https://doi.org/10.1126/science.1195223>
- Caporaso, J. G., Lauber, C. L., Walters, W. A., Berg-Lyons, D., Lozupone, C. A., Turnbaugh, P. J., et al. (2011). Global patterns of 16S rRNA diversity at a depth of millions of sequences per sample. *Proceedings of the National Academy of Sciences*, 108(Supplement 1), 4516–4522. <https://doi.org/10.1073/pnas.1000080107>
- Chan, E. W., Kessler, J. D., Shiller, A. M., Joung, D. J., & Colombo, F. (2016). Aqueous Mesocosm Techniques Enabling the Real-Time Measurement of the Chemical and Isotopic Kinetics of Dissolved Methane and Carbon Dioxide. *Environmental Science & Technology*, 50(6), 3039–3046. <https://doi.org/10.1021/acs.est.5b04304>
- Chan, E. W., Shiller, A. M., Joung, D. J., Arrington, E. C., Valentine, D. L., Redmond, M. C., et al. (2019). Investigations of Aerobic Methane Oxidation in Two Marine Seep Environments Part 2: Isotopic Kinetics. *Journal of Geophysical Research: Oceans*, 124. <https://doi.org/10.1029/2019JC015603>
- Collier, R. W. (1985). Molybdenum in the northeast Pacific Ocean. *Limnology and Oceanography*, 30(6), 1351–1354. <https://doi.org/10.4319/lo.1985.30.6.1351>
- Crespo-Medina, M., Meile, C. D., Hunter, K. S., Diercks, A.-R., Asper, V. L., Orphan, V. J., et al. (2014). The rise and fall of methanotrophy following a deepwater oil-well blowout. *Nature Geoscience*, 7(6), 423–427. <https://doi.org/10.1038/NGEO2156>
- Culpepper, M. A., & Rosenzweig, A. C. (2012). Architecture and active site of particulate methane monooxygenase. *Critical Reviews in Biochemistry and Molecular Biology*, 47(6), 483–492. <https://doi.org/10.3109/10409238.2012.697865>
- Dalton, H., & Leak, D. J. (1985). Methane oxidation by microorganisms. In R. K. Polle & C. S. Dow (Eds.), *Microbial Gas Metabolism* (pp. 173–200). New York, NY: Academic Press.
- de Angelis, M. A., Lilley, M. D., Olson, E. J., & Baross, J. A. (1993). Methane oxidation in deep-sea hydrothermal plumes of the endeavour segment of the Juan de Fuca Ridge. *Geochimica et Deep Sea Research Part I: Oceanographic Research Papers*, 40(6), 1169–1186. [https://doi.org/10.1016/0967-0637\(93\)90132-M](https://doi.org/10.1016/0967-0637(93)90132-M)
- Dickens, G. R. (2011). Down the Rabbit Hole: toward appropriate discussion of methane release from gas hydrate systems during the Paleocene-Eocene thermal maximum and other past hyperthermal events. *Climate of the Past*, 7(3), 831–846. <https://doi.org/10.5194/cp-7-831-2011>
- Dickens, G. R., O'Neil, J. R., Rea, D. K., & Owen, R. M. (1995). Dissociation of oceanic methane hydrate as a cause of the carbon isotope excursion at the end of the Paleocene. *Paleoceanography*, 10(6), 965–971. <https://doi.org/10.1029/95PA02087>
- Dlugokencky, E. J., Nisbet, E. G., Fisher, R., & Lowry, D. (2011). Global atmospheric methane: budget, changes and dangers. *Philosophical Transactions of the Royal Society of London A: Mathematical, Physical and Engineering Sciences*, 369(1943), 2058–2072. <https://doi.org/10.1098/rsta.2010.0341>
- D'souza, N. A., Subramaniam, A., Juhl, A. R., Hafez, M., Chekalyuk, A., Phan, S., et al. (2016). Elevated surface chlorophyll associated with natural oil seeps in the Gulf of Mexico. *Nature Geoscience*, 9(3), 215–218. <https://doi.org/10.1038/NGEO2631>
- Du, M., & Kessler, J. D. (2012). Assessment of the spatial and temporal variability of bulk hydrocarbon respiration following the Deepwater Horizon oil spill. *Environmental Science & Technology*, 46(19), 10499–10507. <https://doi.org/10.1021/es301363k>
- Dubinsky, E. A., Conrad, M. E., Chakraborty, R., Bill, M., Borglin, S. E., Hollibaugh, J. T., et al. (2013). Succession of hydrocarbon-degrading bacteria in the aftermath of the Deepwater Horizon oil spill in the Gulf of Mexico. *Environmental Science & Technology*, 47(19), 10,860–10,867. <https://doi.org/10.1021/es401676y>
- Fox, B. G., Surerus, K. K., Münck, E., & Lipscomb, J. D. (1988). Evidence for a mu-oxo-bridged binuclear iron cluster in the hydroxylase component of methane monooxygenase, Mössbauer and EPR studies. *Journal of Biological Chemistry*, 263(22), 10,553–10,556.
- Hathorne, E. C., Haley, B., Stichel, T., Grasse, P., Zieringer, M., & Frank, M. (2012). Online preconcentration ICP-MS analysis of rare earth elements in seawater. *Geochemistry, Geophysics, Geosystems*, 13(Q01020). <https://doi.org/10.1029/2011GC003907>
- Higgins, J. A., & Schrag, D. P. (2006). Beyond methane: towards a theory for the Paleocene–Eocene thermal maximum. *Earth and Planetary Science Letters*, 245(3–4), 523–537. <https://doi.org/10.1016/j.epsl.2006.03.009>

- Ho, P., Lee, J., Heller, M., Lam, P., & Shiller, A. M. (2018). The distribution of dissolved and particulate Mo and V along the U.S. GEOTRACES East Pacific Zonal Transect (GP16): the roles of oxides and biogenic particles in their distributions in the oxygen deficient zone and the hydrothermal plume. *Marine Chemistry*, 201, 242–255. <https://doi.org/10.1016/j.marchem.2017.12.003>
- Huang, J., Yu, Z., & Chistoserdova, L. (2018). Lanthanide-Dependent Methanol Dehydrogenases of XoxF4 and XoxF5 Clades Are Differentially Distributed Among Methylophilic Bacteria and They Reveal Different Biochemical Properties. *Frontiers in Microbiology*, 9(1366). <https://doi.org/10.3389/fmicb.2018.01366>
- Joung, D., & Shiller, A. M. (2013). Trace element distributions in the water column near the Deepwater Horizon well blowout. *Environmental Science & Technology*, 47(5), 2161–2168. <https://doi.org/10.1021/es303167p>
- Joye, S. B., MacDonald, I. R., Leifer, I., & Asper, V. (2011). Magnitude and oxidation potential of hydrocarbon gases released from the BP oil well blowout. *Nature Geoscience*, 4(3), 160–164. <https://doi.org/10.1038/NNGEO1067>
- Kalyuzhnaya, M. G., Yang, S., Rozova, O., Smalley, N., Clubb, J., Lamb, A., et al. (2013). Highly efficient methane biocatalysis revealed in a methanotrophic bacterium. *Nature Communications*, 4, 2785. <https://doi.org/10.1038/ncomms3785>
- Karl, D. M., Beversdorf, L., Björkman, K. M., Church, M. J., Martinez, A., & Delong, E. F. (2008). Aerobic production of methane in the sea. *Nature Geoscience*, 1(7), 473–478. <https://doi.org/10.1038/ngeo234>
- Kelley, D. S., & Früh-Green, G. L. (1999). Abiogenic methane in deep-seated mid-ocean ridge environments: Insights from stable isotope analyses. *Journal of Geophysical Research*, 104(B5), 10,439–10,460. <https://doi.org/10.1029/1999jb900058>
- Kessler, J. D., & Chan, E. (2017). Chemical and Isotopic Kinetics of Dissolved Methane and Carbon Dioxide for samples collected in the northern Gulf of Mexico and Atlantic July 2014–April 2015. Distributed by Gulf of Mexico Research Initiative Information and Data Cooperative (GRIIDC), Harte Res. Inst., Texas A&M Univ., Corpus Christi, Corpus Christi, <https://doi.org/10.7266/N7RR1WPX>
- Kessler, J. D., & Reeburgh, W. S. (2005). Preparation of natural methane samples for stable isotope and radiocarbon analysis. *Limnology and Oceanography: Methods*, 3, 408–418. <https://doi.org/10.4319/lom.2005.3.408>
- Kessler, J. D., Valentine, D. L., Redmond, M. C., Du, M., Chan, E. W., Mendes, S. D., et al. (2011). A Persistent Oxygen Anomaly Reveals the Fate of Spilled Methane in the Deep Gulf of Mexico. *Science*, 331(6015), 312–315. <https://doi.org/10.1126/science.1199697>
- Kits, K. D., Klotz, M. G., & Stein, L. Y. (2015). Methane oxidation coupled to nitrate reduction under hypoxia by the Gammaproteobacterium *Methylomonas denitrificans*, sp. nov. type strain FJG1. *Environmental Microbiology*, 17(9), 3219–3232. <https://doi.org/10.1111/1462-2920.12772>
- Kozich, J. J., Westcott, S. L., Baxter, N. T., Highlander, S. K., & Schloss, P. D. (2013). Development of a dual-index sequencing strategy and curation pipeline for analyzing amplicon sequence data on the MiSeq Illumina sequencing platform. *Applied and Environmental Microbiology*, 79(17), 5112–5120. <https://doi.org/10.1128/AEM.01043-13>
- Leonte, M., Kessler, J. D., Kellermann, M. Y., Arrington, E. C., Valentine, D. L., & Sylva, S. P. (2017). Rapid rates of aerobic methane oxidation at the feather edge of gas hydrate stability in the waters of Hudson Canyon, US Atlantic Margin. *Geochimica et Cosmochimica Acta*, 204, 375–387. <https://doi.org/10.1016/j.gca.2017.01.009>
- Mau, S., Bles, J., Helmke, E., Niemann, H., & Damm, E. (2013). Vertical distribution of methane oxidation and methanotrophic response to elevated methane concentrations in stratified waters of the Arctic fjord Storfjorden (Svalbard, Norway). *Biogeosciences*, 10(10), 6267–6278. <https://doi.org/10.5194/bg-10-6267-2013>
- Murrell, J. C., McDonald, I. R., & Gilbert, B. (2000). Regulation of expression of methane monooxygenases by copper ions. *Trends in Microbiology*, 8(5), 221–225. [https://doi.org/10.1016/S0966-842X\(00\)01739-X](https://doi.org/10.1016/S0966-842X(00)01739-X)
- EV Nautilus (2015). Explosive Methane Burst and Bubble Streams|Nautilus Live, edited by EVNautilus, YouTube. [https://youtu.be/pO\\_rXOEWnAA](https://youtu.be/pO_rXOEWnAA)
- Oremland, R. S., & Taylor, B. F. (1978). Sulfate reduction and methanogenesis in marine sediments. *Geochimica et Cosmochimica Acta*, 42(2), 209–214. [https://doi.org/10.1016/0016-7037\(78\)90133-3](https://doi.org/10.1016/0016-7037(78)90133-3)
- Pack, M. A., Heintz, M. B., Reeburgh, W. S., Trumbore, S. E., Valentine, D. L., Xu, X., & Druffel, E. R. M. (2015). Methane oxidation in the eastern tropical North Pacific Ocean water column. *Journal of Geophysical Research: Biogeosciences*, 120, 1078–1092. <https://doi.org/10.1002/2014JG002900>
- Picone, N., & Op den Camp, H. J. M. (2019). Role of rare earth elements in methanol oxidation. *Current Opinion in Chemical Biology*, 49, 39–44. <https://doi.org/10.1016/j.cbpa.2018.09.019>
- Pol, A., Barends, T. R. M., Dietl, A., Khadem, A. F., Eygensteyn, J., Jetten, M. S. M., & Op den Camp, H. J. M. (2014). Rare earth metals are essential for methanotrophic life in volcanic mudpots. *Environmental Microbiology*, 16(1), 255–264. <https://doi.org/10.1111/1462-2920.12249>
- Quayle, J. R., & Ferenci, T. (1978). Evolutionary aspects of autotrophy. *Microbiological Reviews*, 42(2), 251–273.
- Raghoebarsing, A. A., Pol, A., van de Pas-Schoonen, K. T., Smolders, A. J. P., Ettwig, K. F., Rijpstra, W. I. C., et al. (2006). A microbial consortium couples anaerobic methane oxidation to denitrification. *Nature*, 440(7086), 918–921. <https://doi.org/10.1038/nature04617>
- Reddy, C. M., Arey, J. S., Seewald, J. S., Sylva, S. P., Lemkau, K. L., Nelson, R. K., et al. (2012). Composition and fate of gas and oil released to the water column during the Deepwater Horizon oil spill. *Proceedings of the National Academy of Sciences*, 109(50), 20,229–20,234. <https://doi.org/10.1073/pnas.1101242108>
- Redmond, M. C., & Valentine, D. L. (2012). Natural gas and temperature structured a microbial community response to the Deepwater Horizon oil spill. *Proceedings of the National Academy of Sciences*, 109(50), 20,292–20,297. <https://doi.org/10.1073/pnas.1108756108>
- Redmond, M. C., Valentine, D. L., & Sessions, A. L. (2010). Identification of novel methane-, ethane-, and propane-oxidizing bacteria at marine hydrocarbon seeps by stable isotope probing. *Applied and Environmental Microbiology*, 76(19), 6412–6422. <https://doi.org/10.1128/AEM.00271-10>
- Reeburgh, W. S. (2007). Oceanic methane biogeochemistry. *Chemical Reviews*, 107(2), 486–513. <https://doi.org/10.1021/cr050362v>
- Rivers, A. R., Sharma, S., Tringe, S. G., Martin, J., Joye, S. B., & Moran, M. A. (2013). Transcriptional response of bathypelagic marine bacterioplankton to the Deepwater Horizon oil spill. *ISME Journal*, 7(12), 2315–2329. <https://doi.org/10.1038/ismej.2013.129>
- Rogener, M. K., Bracco, A., Hunter, K. S., Saxton, M. A., & Joye, S. B. (2018). Long-term impact of the Deepwater Horizon oil well blowout on methane oxidation dynamics in the northern Gulf of Mexico. *Elementa-Science of the Anthropocene*, 6(73). <https://doi.org/10.1525/elementa.332>
- Rona, P., Guida, V., Scranton, M., Gong, D., Macelloni, L., Pierdomenico, M., et al. (2015). Hudson submarine canyon head offshore New York and New Jersey: A physical and geochemical investigation. *Deep-Sea Research Part II-Topical Studies in Oceanography*, 121(S1), 213–232. <https://doi.org/10.1016/j.dsr2.2015.07.019>
- Ross, M. O., MacMillan, F., Wang, J., Nisthal, A., Lawton, T. J., Olafson, B. D., et al. (2019). Particulate methane monooxygenase contains only monocopper centers. *Science*, 364(6440), 566–570. <https://doi.org/10.1126/science.aav2572>

- Ruppel, C. D., & Kessler, J. D. (2017). The Interaction of Climate Change and Methane Hydrates. *Reviews of Geophysics*, 55(1), 126–168. <https://doi.org/10.1002/2016RG000534>
- Ryerson, T. B., Camilli, R., Kessler, J. D., Kujawinski, E. B., Reddy, C. M., Valentine, D. L., et al. (2012). Chemical data quantify Deepwater Horizon hydrocarbon flow rate and environmental distribution. *Proceedings of the National Academy of Sciences*, 109(50), 20,246–20,253. <https://doi.org/10.1073/pnas.1110564109>
- Sherwood Lollar, B., Westgate, T., Ward, J., Slater, G., & Lacrampe-Couloume, G. (2002). Abiogenic formation of alkanes in the Earth's crust as a minor source for global hydrocarbon reservoirs. *Nature*, 416(6880), 522–524. <https://doi.org/10.1038/416522a>
- Shiller, A. M., Chan, E. W., Joung, D. J., Redmond, M. C., & Kessler, J. D. (2017). Light rare earth element depletion during Deepwater Horizon blowout methanotrophy. *Scientific Reports*, 7(1), 10389. <https://doi.org/10.1038/s41598-017-11060-z>
- Shiller, A. M., & Joung, D. J. (2012). Nutrient depletion as a proxy for microbial growth in Deepwater Horizon subsurface oil/gas plumes. *Environmental Research Letters*, 7(4), 045301. <https://doi.org/10.1088/1748-9326/7/4/045301>
- Sirajuddin, S., & Rosenzweig, A. C. (2015). Enzymatic Oxidation of Methane. *Biochemistry*, 54(14), 2283–2294. <https://doi.org/10.1021/acs.biochem.5b00198>
- Skarke, A., Ruppel, C., Kodis, M., Brothers, D., & Lobecker, E. (2014). Widespread methane leakage from the sea floor on the northern US Atlantic margin. *Nature Geoscience*, 7(9), 657–661. <https://doi.org/10.1038/NGEO2232>
- Socolofsky, S. A., Adams, E. E., & Sherwood, C. R. (2011). Formation dynamics of subsurface hydrocarbon intrusions following the Deepwater Horizon blowout. *Geophysical Research Letters*, 38, L09602. <https://doi.org/10.1029/2011GL047174>
- Valentine, D. L. (2011). Emerging topics in marine methane biogeochemistry. *Annual Review of Marine Science*, 3, 147–171. <https://doi.org/10.1146/annurev-marine-120709-142734>
- Valentine, D. L., Blanton, D. C., Reeburgh, W. S., & Kastner, M. (2001). Water column methane oxidation adjacent to an area of active hydrate dissociation. Eel River Basin. *Geochimica et Cosmochimica Acta*, 65(16), 2633–2640. [https://doi.org/10.1016/S0016-7037\(01\)00625-1](https://doi.org/10.1016/S0016-7037(01)00625-1)
- Valentine, D. L., Kessler, J. D., Redmond, M. C., Mendes, S. D., Heintz, M. B., Farwell, C., et al. (2010). Propane Respiration Jump-Starts Microbial Response to a Deep Oil Spill. *Science*, 330(6001), 208–211. <https://doi.org/10.1126/science.1196830>
- Valentine, D. L., Mezić, I., Mačević, S., Črnjarić-Žic, N., Ivić, S., Hogan, P. J., et al. (2012). Dynamic autoinoculation and the microbial ecology of a deep water hydrocarbon irruption. *Proceedings of the National Academy of Sciences*, 109(50), 20,286–20,291. <https://doi.org/10.1073/pnas.1108820109>
- Voss, M., Bange, H. W., Dippner, J. W., Middelburg, J. J., Montoya, J. P., & Ward, B. (2013). The marine nitrogen cycle: recent discoveries, uncertainties and the potential relevance of climate change. *Philosophical Transactions of the Royal Society B: Biological Sciences*, 368(1621), 20130121. <https://doi.org/10.1098/rstb.2013.0121>
- Waki, M., Tanaka, Y., Osada, T., & Suzuki, K. (2002). Effects of nitrite and ammonium on methane-dependent denitrification. *Applied Microbiology and Biotechnology*, 59(2-3), 338–343. <https://doi.org/10.1007/s00253-002-1003-y>
- Wear, E. K., Carlson, C. A., Windecker, L. A., & Brzezinski, M. A. (2015). Roles of diatom nutrient stress and species identity in determining the short- and long-term bioavailability of diatom exudates to bacterioplankton. *Marine Chemistry*, 177(2), 335–348. <https://doi.org/10.1016/j.marchem.2015.09.001>
- Weinstein, A., Navarrete, L., Ruppel, C., Weber, T. C., Leone, M., Kellermann, M. Y., et al. (2016). Determining the flux of methane into Hudson Canyon at the edge of methane clathrate hydrate stability. *Geochemistry, Geophysics Geosystems*, 17(10), 3882–3892. <https://doi.org/10.1002/2016GC006421>
- Weiss, R. F. (1974). Carbon dioxide in water and seawater: the solubility of a non-ideal gas. *Marine Chemistry*, 2(3), 203–215. [https://doi.org/10.1016/0304-4203\(74\)90015-2](https://doi.org/10.1016/0304-4203(74)90015-2)
- Wiesenburg, D. A., & Guinasso, N. L. Jr. (1979). Equilibrium solubilities of methane, carbon monoxide, and hydrogen in water and sea water. *Journal of Chemical and Engineering Data*, 24(4), 356–360. <https://doi.org/10.1021/jc60083a006>
- Yvon-Lewis, S. A., Hu, L., & Kessler, J. (2011). Methane flux to the atmosphere from the Deepwater Horizon oil disaster. *Geophysical Research Letters*, 38, L01602. <https://doi.org/10.1029/2010gl045928>
- Zeebe, R. E., Ridgwell, A., & Zachos, J. C. (2016). Anthropogenic carbon release rate unprecedented during the past 66 million years. *Nature Geoscience*, 9(4), 325–329. <https://doi.org/10.1038/NGEO2681>